



## Cosmic ray helium isotopes from the BESS-Polar I experiment

N. PICOT-CLEMENTE<sup>1</sup>, K. ABE<sup>2</sup>, H. FUKU<sup>3</sup>, S. HAINO<sup>4</sup>, T. HAMS<sup>5</sup>, A. ITAZAKI<sup>2</sup>, K.C. KIM<sup>1</sup>, T. KUMAZAWA<sup>4</sup>, M.H. LEE<sup>1</sup>, Y. MAKIDA<sup>4</sup>, S. MATSUDA<sup>4</sup>, K. MATSUMOTO<sup>4</sup>, J.W. MITCHELL<sup>5</sup>, Z. MYERS<sup>5</sup>, J. NISHIMURA<sup>6</sup>, M. NOZAKI<sup>4</sup>, R. ORITO<sup>2</sup>, J.F. ORMES<sup>7</sup>, M. SASAKI<sup>5</sup>, E.S. SEO<sup>1</sup>, Y. SHIKAZE<sup>2</sup>, R.E. STREITMATTER<sup>5</sup>, J. SUZUKI<sup>4</sup>, Y. TAKASUGI<sup>2</sup>, K. TAKEUCHI<sup>2</sup>, K. TANAKA<sup>4</sup>, T. YAMAGAMI<sup>3</sup>, A. YAMAMOTO<sup>4</sup>, T. YOSHIDA<sup>3</sup>, K. YOSHIMURA<sup>4</sup>

<sup>1</sup> IPST, University of Maryland, College Park MD 20742, USA

<sup>2</sup> Kobe University, Kobe, Hyogo 657-8501, Japan

<sup>3</sup> ISAS/JAXA, Sagamihara, Kanagawa 252-5210, Japan

<sup>4</sup> KEK, Tsukuba, Ibaraki 305-0801, Japan

<sup>5</sup> NASA/GSFC, Greenbelt, MD 20771, USA

<sup>6</sup> The University of Tokyo, Bunkyo, Tokyo 113-0033, Japan

<sup>7</sup> University of Denver, Denver, CO 80208, USA

picot@umd.edu

**Abstract:** The first flight of the Balloon-Borne Experiment with a Superconducting Spectrometer (BESS-Polar I) in Antarctica collected about 900 million cosmic ray events during 8.5 days in 2004. Particle charge was determined from energy loss in the scintillators, rigidity by reconstructing each particle trajectory in the magnetic field, and velocity by utilizing time of flights counters. These measurements can clearly identify hydrogen and helium isotopes among the incoming particles. These isotopes are generally believed to result from nuclear interactions of primaries with the interstellar medium. Measurement of their flux is expected to provide important information on cosmic ray sources and particle propagation in interstellar space. The presentation will focus on determination of the helium isotope flux in the kinetic energy per nucleon range 0.1 GeV/n to about 1.5 GeV/n. After quickly introducing the BESS-Polar I detector, the dedicated analysis to differentiate isotopes will be described. Finally, the energy spectra will be presented and compared to previous measurements.

**Keywords:** BESS, BESS-Polar I, helium isotopes, cosmic-rays, balloon-borne experiment

## 1 Introduction

Between 1993 and 2002, the BESS collaboration carried out 9 successful missions in northern Canada [1, 2, 3]. Then, in order to improve the sensitivity for low energy particles by taking advantage of a lower geomagnetic cutoff, and improve the exposure time, the long-duration balloon flight BESS-Polar was developed [4, 5, 6]. The first detector BESS-Polar I was sent in Antarctica in 2004 for 8.5 days of data taking, whereas the second flight was sent in 2007 for 20 days of data taking.

The BESS experiment is aimed to study elementary particle phenomena in the early history of the Universe by measuring precisely low energy antiprotons, and searching for antiparticles in the cosmic rays [7, 8, 9, 10]. Moreover, the BESS instruments allow to measure isotopes of hydrogen and helium nuclei. These measurements give complementary information on the solar modulation, as well as provide information on the cosmic-ray origin and propagation history in interstellar space.

This paper will be focused on the spectra determination of helium isotopes with the BESS-Polar I detector. After having described the instruments in section §2, the different steps needed for getting the spectra will be detailed in section §3.

## 2 The BESS-Polar I detector

As shown in fig. 1, the BESS-Polar I components were concentrically arranged. From the top to the bottom, which corresponds to the crossing of a downward going particle, the detector contains an upper plastic scintillator hodoscope (TOF), a solenoidal superconducting magnet producing a uniform magnetic field of 0.8 T and surrounding two layers of inner drift chambers, a central jet-type drift chamber and a middle TOF. It is finally composed by an aerogel Cherenkov counter and a lower TOF.

The implementation of the middle TOF, as well as the reduction of the material inside the detector down to 5 g.cm<sup>-2</sup> are the main differences between previous BESS

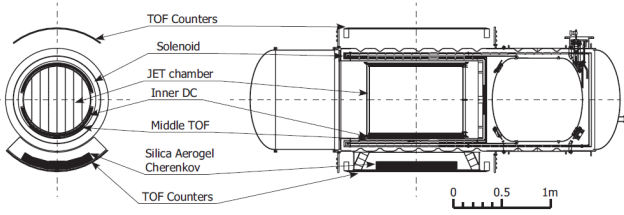


Figure 1: Cross section of the BESS-Polar I detector.

spectrometers. These modifications allowed the experiment to improve the sensitivity to low energy particles from about 0.1 GeV/n. The use of a cylindrical configuration gives a large geometrical acceptance while keeping a compact size for the detector. Thanks to the field uniformity and the configuration, the detector performance is almost identical with various hit positions and incident angles, which is essential for a reliable absolute flux determination. More details on the BESS-Polar I detector can be found in paper [11].

### 3 Analysis

The analysis is divided in 4 different steps. The first step consists in extracting the particle characteristics from the BESS-Polar I instruments. Then, in the second step, by studying the response of the detector and of the track reconstruction algorithm to the crossing of simulated particles, cuts are defined in order to remove events having interacted hadronically in the detector, and to keep only those for which the path of the reconstructed track is included inside the detector volume, with good quality parameters. In the third step, cuts are applied to real data, and from the measured particle mass distributions and the energy resolution of the experiment, the numbers of helium 3 and helium 4 events are extracted. Finally, by knowing the cut efficiencies with the use of MonteCarlo data, the number of events remaining in real data, and by estimating the number of secondaries created in the upper atmosphere, the energy spectra is calculated.

For the analysis, MonteCarlo simulations were performed.  $10^8$  helium 3 and helium 4 events were equally generated on a demi-sphere above the detector, and randomly in the kinetic energy range per nucleon 0.0025 to 6.2500 GeV/n.

#### 3.1 Particle characteristics from BESS instruments

The Time-Of-Flight hodoscopes (TOF) and the tracker of the BESS polar detector constitute complementary instruments for the determination of the charge and the mass of the incoming particle. The use of two different layers of TOFs gives an information on the velocity of the particle. A good measurement is achieved thanks to a time resolution of about 110 ps, which yield to a resolution on the

velocity of about 3 %. Such a resolution is primordial for the charge and mass determination. Indeed, by using the relation

$$\frac{dE}{dX} = \left(\frac{Z}{\beta}\right)^2 f(\beta), \quad (1)$$

which describes the energy loss per length unit  $\frac{dE}{dX}$  for a particle of velocity  $\beta$  crossing a TOF, its charge  $Z$  can be extracted after having determined the function  $f(\beta)$  from MonteCarlo simulation. The fig. 2 shows the distribution of charge obtained by using MonteCarlo simulations for helium events crossing the Upper and Lower TOFs. Also shown is the distribution of charge obtained for proton events with the detector. A good reconstruction of charge is reached with the instrument.

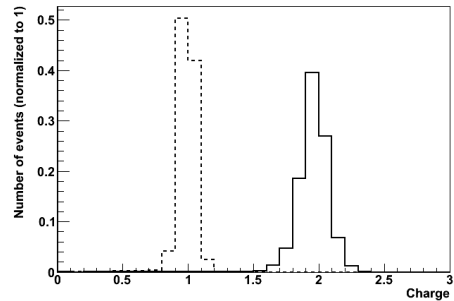


Figure 2: Distribution of charge for MonteCarlo simulated helium events (full line) and proton events (dashed line).

From the reconstruction of the particle trajectory inside the detector, by using hits in TOFs and the tracker, the gyro-radius  $\rho$  of the incoming particle deviated by the magnetic field  $B$  is determined, and then its rigidity  $R$  from the relation

$$R = \rho/B. \quad (2)$$

Thus, the mass  $M$  of the particle relied to its charge, its rigidity and its velocity can be calculated with the formula

$$M = ZR\sqrt{1/\beta - 1}. \quad (3)$$

The distributions of reconstructed mass for particles of helium 3 and helium 4, as well as hydrogens and deuterons, coming from MonteCarlo simulations with energies lower than 250 MeV/n are shown in fig. 3. Distributions are well centered on their corresponding expected mass values with good resolutions of mass, increasing with the increasing mass.

Finally for a full knowledge of the crossing particle, its kinetic energy per nucleon  $E_k$  can be determined from the relation

$$E_k = \sqrt{R^2 Z_t^2 + M_t^2} - M_t. \quad (4)$$

It has to be noticed that  $Z_t$  and  $M_t$  are imposed accordingly to the researched particle, they mean the true value of charge and mass for the particle. Thus, for example when searching for helium events,  $Z_t$  will be set to 2, and

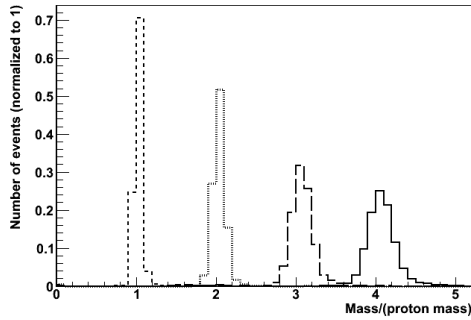


Figure 3: Distribution of mass for MonteCarlo simulated helium 3 (long-dashed line) and helium 4 (full line) events, as well as for hydrogens (dashed line) and deuterons (dotted).

the mass  $M_t$  will be  $2.81 \text{ GeV}/c^2$  for helium 3 and  $3.73 \text{ GeV}/c^2$  for helium 4. To this calculated kinetic energy is then taken into account the estimated energy losses in the detector from the reconstructed path of the particle, and in the atmosphere. The energy resolution obtained is less than  $0.04 \text{ GeV}/n$ , and is smaller than the energy bins used in the analysis.

### 3.2 Selection of “good” events

In such analysis, to calculate the absolute flux, the use of particles without hadronic interactions in the detector and with correct measurements is required. After having asked trivial conditions, such as keeping only downward going reconstructed particles with positive reconstructed rigidities, this purpose is achieved by applying several selection criteria, separated here within 4 categories:

- The selection of non-interacting events: Events which interacts hadronically in the detector can be easily removed from the sample. Indeed their signature is often characterized by several hits produced in TOFs, as well as in the JET chamber, but also by several reconstructed tracks, and reconstructed tracks for which the expected hits in the detector doesn't match the real ones. All these different criteria were studied, and a bunch of cuts was finally defined from MonteCarlo distributions, for a final efficiency on non-interacting events of about 98 %.
- The selection of non-border particles: Particles passing through the sides of the instruments, such as TOFs or the tracking chamber will be much likely badly reconstructed than events crossing the center of the detector. Conditions were thus applied to avoid to keep such events, and the resulted energy independent selection efficiency is of about 70 % for a kinetic energy per nucleon higher than  $0.1 \text{ GeV}/n$ .
- The selection of good quality events: In order to reach good mass, charge and thus energy measurements, good quality events need to be selected. The

main selection consists in applying conditions on the fit quality, called chisquares, after having studied carefully MonteCarlo distributions. Also, to ensure that the particle cross the center of the tracker, the combination between left (right) edge upper TOF counter and left (right) edge lower counter are removed by cutting events with the shortest path lengths. Finally, the most stringent criteria in this step is the ask for a number of detected hits in the tracking chamber higher than 60 % of the number of expected hits. This condition allows to remove the tracking failure events which have good quality fits due to the reconstruction with exclusive hits association in the JET chamber. The quality selection efficiency obtained is of about 40 % for helium 3 events, as well as for helium 4.

- The selection of helium events: In order to discriminate helium from proton events, this step consists in applying a cut on the measured charge of the particle. This measured charge is proportionnal to the energy loss per length unit in TOFs. The fig. 4 illustrates the energy loss per centimeter as a function of the measured rigidity of the incoming particle for a sample of 10 % of the whole real dataset. A valley determined by the use of a simple algorithm and fitted from the relation (3) is represented by the dashed line, which shows the separation cut between protons below and heliums above. Finally the fitted curve is employed to separate proton from helium events, with an efficiency get from MonteCarlo simulations of about 90 %.

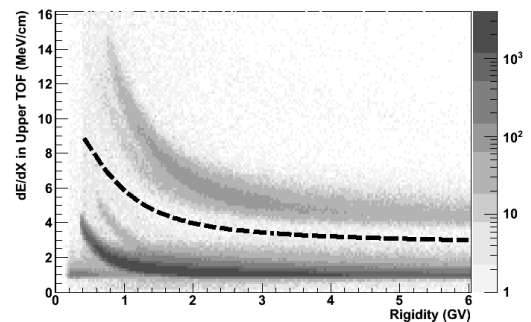


Figure 4: Energy loss per centimeter as a function of the measured rigidity of the incoming particle for a sample of 10 % of the whole real dataset. The dashed line represents the separation cut between hydrogens below and heliums above.

### 3.3 Determination of the number of helium 3 and helium 4 events

Once the definition of the selection cuts performed, the latter are applied to the real data. The distributions of mass are then displayed for several ranges of kinetic energy per nucleon and fitted by two gaussians in order to extract the

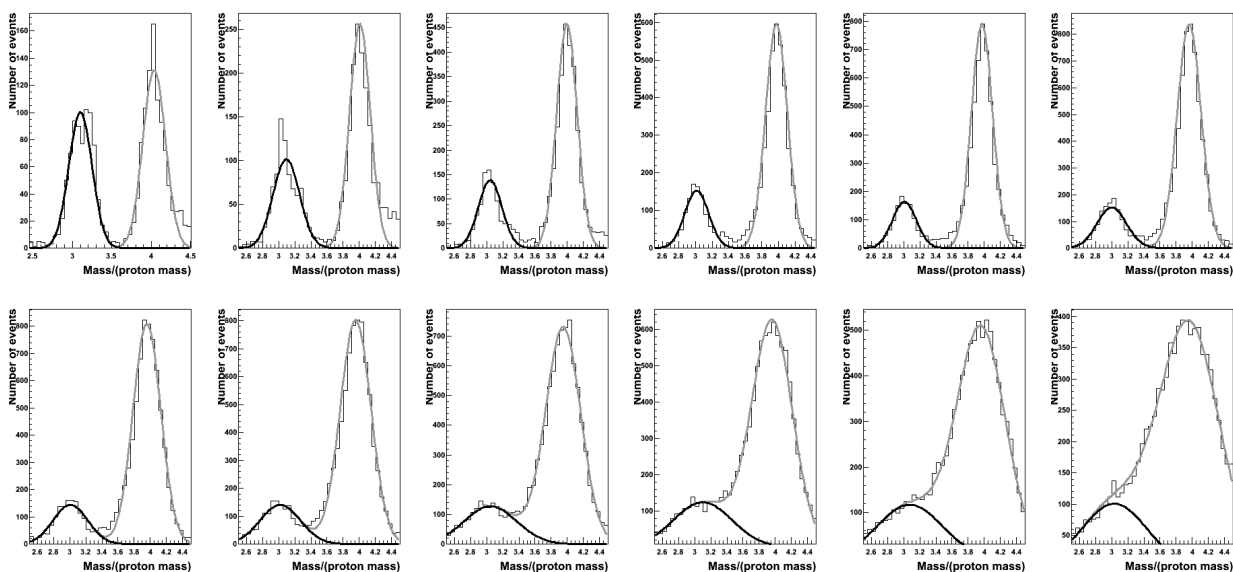


Figure 5: Mass distributions for a sample of 10 % of the whole real dataset for several bins of kinetic energy per nucleon, as well as the corresponding fits, when extracting helium 3 events. Are shown distributions for kinetic energies per nucleon, in the top from the left to the right, of  $0.148 \leq Ekn < 0.182$  GeV/n,  $0.182 \leq Ekn < 0.224$  GeV/n,  $0.224 \leq Ekn < 0.275$  GeV/n,  $0.275 \leq Ekn < 0.338$  GeV/n,  $0.338 \leq Ekn < 0.416$  GeV/n,  $0.416 \leq Ekn < 0.512$  GeV/n, and in the bottom from the left to the right, of  $0.512 \leq Ekn < 0.630$  GeV/n,  $0.630 \leq Ekn < 0.775$  GeV/n,  $0.775 \leq Ekn < 0.953$  GeV/n,  $0.953 \leq Ekn < 1.173$  GeV/n,  $1.173 \leq Ekn < 1.443$  GeV/n and  $1.443 \leq Ekn < 1.775$  GeV/n.

signal of helium 3 and helium 4 events. In fig. 5 are shown examples of mass distributions for several bins of kinetic energy per nucleon, as well as the corresponding fits, when extracting helium 3 events from a sample of 10 % of the whole real dataset. Below about 0.1 GeV/n statistics are not sufficient for extrapolating helium events, notably because of too many particles stopped inside the detector. And finally, above about 1.5 GeV/n distributions of mass for helium 3 and helium 4 become too close to perform a good identification of the particles.

### 3.4 Calculation of the energy spectra

Before calculating the absolute energy spectra of helium isotopes, two contributions need to be taken into account. The number of events  $N_{fit}$ , for every bins of energy, extracted from the fits performed on mass distributions, contains a percentage of events for which the energy is badly reconstructed. In order to estimate this fraction  $\epsilon_{reco}$ , MonteCarlo simulations are employed, and the number of remaining events reconstructed in their good energy range is divided by the total number of remaining events. The percentage is a function of the energy resolution and the chosen energy bins, and will decrease with a worse resolution or with the choice of lower ranges of energy. With the current choice of bins, the MonteCarlo study shows that about 90% of the remaining events have a good reconstructed energy.

The second contribution to be taken into account is the number of helium events which are secondaries instead of primaries. To estimate this number, interactive loop cal-

culations among several particles are performed. These iterations are then stopped when the resulting flux obtained matches the flux at the top of instrument, and the number of measured secondaries  $N_{sec}$  is thus deduced.

Finally, the absolute flux of helium 3 and helium 4 can be separately calculated from the formula

$$\phi = \frac{(N_{fit} - N_{sec}) \times \epsilon_{reco}}{\epsilon_{tot} \times A_{eff} \times T \times E_{bin}}, \quad (5)$$

where  $\epsilon_{tot}$  is the total cut efficiency,  $A_{eff}$  the effective area of the detector,  $T$  the total time of data taking, and  $E_{bin}$  the range of the kinetic energy bin.

## References

- [1] Y. Ajima et al., Nucl. Instr. & Meth. A 443, 71 (2000)
- [2] S. Orito, ASTROMAG Workshop, KEK Report 87-19, 111 (1987)
- [3] A. Yamamoto et al., Adv. Space Res., 14, 2, 75 (1994)
- [4] A. Yamamoto et al., Adv. Space Res. 33 (5) 1253 (2002)
- [5] J. W. Mitchell et al., Nucl. Phys. B (Proc. Suppl.) 134 (2004) 31
- [6] T. Yoshida et al., Adv. Space Res. 33 (10) 1755 (2004)
- [7] J. Z. Wang et al., 27th ICRC, Hamburg (2001) 5, 1671
- [8] H. Fuke et al., Phys. Rev. Lett. 95, 081101 (2005)
- [9] Z. D. Myers et al., Adv. Space Res., 35, 151 (2005)
- [10] Y. Shikaze et al., Astroparticle Phys., 28, 154 (2007)
- [11] K. Abe et al., Phys. Lett. B, 670, 103 (2008)